Low-dose irradiation promotes bone regeneration through osteoblasts proliferation and M2 polarization of macrophages

Shaoqing Chen
The Affiliated Changzhou No 2 People's Hospital of Nanjing Medical University https://orcid.org/0000-0002-4890-512X
Su Ni
The Affiliated Changzhou No 2 People's Hospital of Nanjing Medical University
Chun Liu
The Affiliated Changzhou No 2 People's Hospital of Nanjing Medical University
Mu He
The Affiliated Changzhou No 2 People's Hospital of Nanjing Medical University
Yiwen Pan
The Affiliated Changzhou No 2 People's Hospital of Nanjing Medical University
Pengfei Cui
Changzhou University
Cheng Wang
Changzhou University
Xinye Ni (nxy@njmu.edu.cn)

Research

Keywords: Irradiation, Macrophage polarity, Osteoblast proliferation, Bone regeneration

Posted Date: June 3rd, 2022

DOI: https://doi.org/10.21203/rs.3.rs-1670025/v1

Abstract

Background: Current studies still have a controversy on the effect and doses of irradiation (IR) on bone regeneration. Moreover, the mechanisms of IR to bone regeneration mainly focus on the direct effects on osteoblasts, with neglect to the role of the surrounding immune environment. Our purpose was to explore the effect of IR on osteoblasts proliferation and macrophages polarity.

Results: Here in this study, we firstly established the rat cranial defects model and revealed that low-dose IR≤2 Gy gradually promoted bone regeneration, while high-dose IR>2Gy inhibited bone regeneration. The change of macrophage polarity in peripheral blood samples showed that low-dose IR≤2 Gy triggered M2 polarization of macrophages, high-dose IR>2 Gy led to M1 polarization. The cellular level also showed the similar results, mouse leukemia cells of monocyte macrophages cells (Raw264.7) exhibited M2 polarization under low-dose IR≤2 Gy, and M1 polarization under high-dose IR>2Gy. Furthermore low-dose IR≤2 Gy promoted the proliferation of osteoblasts, while high-dose IR>2 Gy exhibited the opposite result. The co-culture results showed that low-dose IR≤2 Gy not only promoted bone regeneration through osteoblasts proliferation, but also promoted bone regeneration through M2 polarization of Raw264.7 cells, while high-dose IR>2 Gy had the opposite effect.

Conclusions: Our findings have revealed that low-dose IR≤2 Gy promotes bone regeneration by indirectly promoting macrophage M2 polarization and direct osteoblast proliferation, while high-dose IR>2 Gy has the opposite effect, which might offer inspirations for the related studies.

1. Background

It has been common sense in the scientific community that high-dose ionizing irradiation (IR) can deliver deleterious effects to bone tissue. [1–3] The subjects can suffer from significant osteoradionecrosis, sclerosis and even a high incidence of bone fracture. [4–7] The osteoblasts critical for the maintenance of normal bone functions are demonstrated to show impaired proliferation and differentiation after high-dose IR. Further explorations have also revealed that increased cell-cycle arrest, reduced collagen production and acquired vulnerability to apoptotic agents are responsible for the damage caused high-dose IR. [8, 9] However, the effects of low-dose IR on the bone tissues, especially bone repair, have not been fully explored by previous studies. Instead of high-dose IR, low-dose IR such as radiography, computed tomography or fluoroscopy during surgery, is more common occurred to patients, especially those subjected to orthopedic operations and with bone fractures. [10–12] Therefore, understanding whether low-dose IR also has the same impact on patients through the same or similar mechanisms is an important issue for those suffering from the bone defect that needs frequent low-dose IR.

Unfortunately, there are remaining controversies among previous researches on the effects of low-dose IR and its underlying mechanisms. Wright et al. reported that 2 Gy of IR could result in local and systemic bone loss in C57BL/6 mice. [13] Chen et al., showed that 0.5 Gy of IR promoted the fracture repair in Sprague Dawley (SD) rats. [14] In the work of Hu et al., X-ray at 2 Gy decreased the mineralization effect

of OCT-1 cells after a single IR. [15] In contrast, the same cell line subjected to the same dose exerted only time-dependent cell cycle arrest without significant effects on the proliferation and differentiation effect [8], while another study further suggested that 2 Gy of X-ray not only increased differentiation and mineralization potential of calvarial osteoblasts but also upregulated the expression of many related cytokines, including alkaline phosphatase (ALP), osteopontin (OPN), and osteocalcin (OCN) during the process. [16] As these previous studies were performed using different animal models, IR source/dose, exposure method and cell lines, further evidence should be added to draw a more comprehensive profile on the effect of IR on bone repair and its underlying mechanisms.

In addition to the debates on this issue, there are still shortages of previous studies that mainly focus on the direct impact of IR with restriction to the proliferation of osteoclast or osteoblast. However, the immune environment in bone tissue constituted by a variety of cells, which collectively create a microenvironment to afford orchestrated bone remodeling. The significance of the immune environment in bone tissue is drawing more and more attention. Macrophages, as a critical component of the innate immune system, are demonstrated to exert important regulatory roles in bone homeostasis and repair. [17, 18] It was reported that bone repair is positively associated with M2 macrophage function [19], and regulated M2 macrophages showed a preventive effect on bone loss in murine periodontitis models. [20] Recently, regulated M2 macrophage polarization using scaffold implantation or exosome was found to significantly enhance bone formation or inhibit periodontal bone loss in animal models. [21, 22]

Here in this study, we studied the effect of varioust doses of IR on bone repair in rats with cranial defects. Then the effect of high- and low-dose IR on the polarity changes of macrophages in rats and *in vitro* was investigated. Meanwhile, we also investigated the effect of various doses of IR on the proliferation of rat bone marrow mesenchymal stem cells (BMSCs). In addition, the effects of IR-induced BMSCs proliferation and Raw264.7 polarity changes on the osteogenesis of BMSCs were explored.

2. Results

2.1 The low dose of IR promotes bone regeneration in rat cranial defect model

To study the effect of IR on bone repair, the rat cranial defect model was firstly established, and rats were subjected to different doses (0, 0.5, 1, 2, 4 Gy) of IR the next day. At 28 days post IR, micro-CT was employed to analyze the formation of new bones within the defect region. As shown in Fig. 1, the 3D-reconstruction of the cranium in different groups (Fig. 1A) revealed that when the IR dose was ≤ 2 Gy, as the IR dose increased, the repair of the cranial defect was better, and the new bone formation increased, a large amount of new bone formation could be seen in the 2 Gy group. In comparison, when the IR dose continued to increase to 4 Gy, it had no effect on bone repair, and no regeneration was observed along the edge of the defect. These observations were also verified by the sagittal view of rat cranial defect in Fig. 1B. Quantification results demonstrated that there was more bone volume in the 2 Gy group than that in other groups (Fig. 1C). Meanwhile, as shown in Fig. 1D, the 2 Gy group had the highest trabecular

thickness than other groups. The micro-CT results indicate that low-dose IR ≤ 2 Gy promotes bone repair, while high-dose IR > 2 Gy has no noticeable effect on bone repair.

2.2 The low dose of IR increases RUNX2 levels in rat cranial defect model

To investigate the expression of osteogenic markers following IR, immunohistochemical staining of runt-related transcription factor 2 (RUNX2) was performed on the cranial samples. As shown in Fig. 2, when the IR dose was ≤ 2 Gy, positive staining at the edge of the defect was increased as the increment of the IR dose, indicating the up-regulated expression of RUNX2 with the increased IR dose. In contrast, further increase of IR dose to 4 Gy resulted in reduced expression of RUNX2. Immunohistochemical staining results reveal the osteoinductive ability of low-dose IR ≤ 2 Gy by upregulating the expression of osteogenic markers, while by contrast, high-dose IR > 2 Gy has no noticeable bone repair effect with no obvious regulating of expression of the osteogenic markers.

2.3 The low dose of IR promotes M2 polarization of macrophage in vivo and in vitro

In order to verify the effect of IR on the polarization of macrophages in cranial defect rats, the orbital blood of rats from different groups at a predetermined time (Day1, 3, 8, 14) were collected to isolate peripheral blood mononuclear cells (PBMC). Then four M1/M2 antibodies, CD80/CD86 for M1-polarized macrophages and CD206/CD163 for M2-polarized macrophages, were stained using corresponding antibodies, followed by CD68 staining for macrophages, and detected by flow cytometry. It showed in Day1 (Fig. 3A), for the low-dose IR ≤ 2 Gy groups, as the IR dose increased, the expression of M1 markers CD80 and CD86 decreased, and the expression of M2 markers CD206 and CD163 increased. When the IR dose continued to increase to 4 Gy, the expression of M1 markers CD80 and CD86 increased, the expression of M2 markers CD206 and CD163 decreased. Day3 and Day8 (Fig. 3B, 3C) showed a similar trend. On Day14, for the low-dose IR ≤ 2 Gy groups, as the IR dose increased, the expression of M1 markers CD80 decreased, CD86 had no significant differences, M2 markers CD206 stayed consistent, and CD163 increased. When the IR dose continued to increase to 4 Gy, the expression of M1 markers CD80 and CD86 increased, M2 markers CD206 had no significant differences, while CD163 decreased. These results indicate that low-dose IR ≤ 2 Gy can reduce the ratio of M1-polarized macrophages and conversely increase that of M2-polarized ones. In contrast, from 2 Gy to 4 Gy, IR reduced the ratio of M2-polarized macrophages but increased that of M1-polarized ones, while by contrast, high-dose IR > 2 Gy exhibits the opposite result.

The effect of IR on the polarization of macrophages in healthy rats was also studied (Figure S1). Healthy rats showed a similar polarization trend as that in cranial defect rats on Day1 and Day3. Interestingly, the irradiated healthy rats showed faster recovery of the changed polarization state (Figure S1) as compared

with the cranial defect model. It was shown that the polarization differences among different groups were started to unify in healthy rats at Day14, and there were almost no differences at Day 28.

To monitor the effect of IR dose on the polarization of macrophages in vitro, Raw264.7 cells were firstly treated with LPS to construct an in vitro inflammation model. Then the cells were subjected to different doses of IR, followed by quantification of mRNA of M1/M2 markers using RT-PCR. iNOS and IL-1 were selected as M1 polarization markers, while BMP2 and CD206 were selected as M2 polarization markers. As shown in Fig. 4, low-dose IR ≤ 2 Gy reduced the expression of M1 polarization-related mRNA and increased the expression of M2 polarization-related mRNA, while high-dose IR > 2 Gy exhibited an opposite result, indicating that low-dose IR ≤ 2 Gy can promote the polarization of macrophages into M2 type, high-dose IR > 2 Gy can promote the polarization of macrophages into M1 type.

2.4 The low dose of IR promotes the proliferation of BMSCs

In order to study the impact of IR doses on the proliferation of BMSCs, the cell viability study and live/dead staining were conducted. After being treated with different doses of IR, BMSCs were allowed to grow for another 24, 48 or 72 h, and the cell viability were monitored using the MTT assay. As shown in Fig. 5A, at 24 h post-IR, there was almost no difference in cell viability among low-dose IR ≤ 2 Gy groups, while the proliferation rate of cells in the 4 Gy group was significantly inhibited. At 48 h, the cell proliferation of the low-dose IR ≤ 2 Gy groups increased slightly, the cell proliferation of the 4 Gy group was significantly inhibited compared with the control group. It was noted that extended incubation time to 72 h showed more significant differences. In particular, BMSCs subjected to 2 Gy IR showed the highest BMSCs proliferation profile and had a significant difference compared to the untreated control group. The 4 Gy group exhibited more apparent differences compared with other groups.

In the live/dead staining assay performed at 72 h post-incubation, as shown in Fig. 5B, the 4 Gy group exhibited some dead/dying cells in the view, while other groups showed high cell viability with almost no dead/dying cells observed, particularly the cell density in the 2 Gy group was the highest among all groups. These results suggests that low-dose IR ≤ 2 Gy promotes the proliferation of BMSCs, while high-dose IR > 2 Gy inhibits the proliferation of BMSCs.

2.5 The low dose of IR-induced osteoblast proliferation and macrophage M2-polarization promote osteogenesis

The osteogenesis differentiation of BMSCs under different treatments were studied. BMSCs were cultured in the osteoblastic induction medium (OIM) and then subjected to different doses of IR, with/without the addition of supernatants of Raw264.7 cells irradiated with corresponding doses of IR. Two osteogenesis factors, ALP and mineralized nodules were selected to reflect the osteogenic differentiation of BMSCs. As shown in Fig. 6A and 7A, low-dose IR ≤ 2 Gy exerted beneficial effects on bone repair as supported by the increased expression of ALP and mineralized nodules in BMSCs, while the 4 Gy group showed decreased expression of ALP and mineralized nodules compared with the OIM group, indicating the high-dose 4 Gy

was not conducive to osteogenesis. Moreover, after being supplied with the supernatants of Raw264.7 cells irradiated with corresponding doses of IR, the level of expression of ALP (Fig. 6B) and mineralized nodules (Fig. 7B) in BMSCs showed more apparent changes. In line with the above observations, the addition of the supernatants of Raw264.7 cells irradiated with low-dose IR significantly promoted the osteogenesis of BMSCs as the IR dose improved. The 2 Gy group showed the best performance with the highest level of ALP/AR staining. Even in the low-dose IR groups, the Raw264.7 supernatant groups exhibited significantly increased staining as the IR dose increased (Fig. 6B, Fig. 7B). In contrast the only irradiated groups had slight increment, indicating that the effect of Raw264.7 polarization to osteogenesis may be stronger than that the effect of cell proliferation. As expected, 4 Gy of IR showed decreased expression of both ALP and mineralized nodules in BMSCs, suggesting the negative effect of high-dose IR in bone repair.

3. Discussion

Based on the fact that IR is a more commonly encountered situation in our daily life, especially those subjected to orthopedic operations and with bone fractures, the effects of IR, including the dose limits and the underlying mechanisms, are urgent to be clarified. In previous studies, the adopted experiment conditions vary from one study to another, which sometimes give contradictive conclusions. To reveal the impact of IR on the repair of bones, in our study, male SD rats with established cranial defects model were employed and subjected to IR of 0.5-4 Gy once, followed by the studying of bone repair at the defect region. The results in Fig. 1 demonstrated that the low-dose IR of 2 Gy showed the best bone regeneration performance. These observations were also in line with previous studies to confirm that low-dose IR can exert a beneficial effect on bone regeneration.

In previous reports, the mechanism studies related to the positive bone regeneration effect of low-dose IR were largely restricted on two targets, osteoblast and osteoclast, since they are directly related to the repair of bones. As bone is a very dynamic tissue, which undergoes continuous remodeling during its lifetime with the coordination of different cells, not only osteoblast and osteoclasts, but also immune cell, with macrophages as one of the most important regulators. Therefore, the impact of low-dose IR on macrophages and the following impact on bone repair, as a long-neglected mode of action, should be considered. In recent years, studies have come to a consensus that macrophages subjected to ≤ 1 Gy of IR treatment were likely to become M2 polarization (anti-inflammatory), while > 2 Gy of IR was more prone to enhance M1 polarization (pro-inflammatory) of macrophages. [23, 24] As previous studies also revealed that macrophages reside during all stages of fracture repair, which also contribute significantly to determine the destiny of repair process. [25, 26] In fact, M1 polarization of macrophages, which shifted the inflammatory reaction after injury towards a pro-inflammatory scenario, usually delays or even impairs successful repair. [27] In contrast, M2 polarization of macrophages could improve the repair outcome with reduced recuperation time. [28, 29] Therefore, there is a high potential that low-dose IR can indirectly navigate the bone repair process by affecting macrophages polarization. Therefore, the M1/M2 polarization profile of macrophage in the circulation was monitored for 14 days using corresponding antibodies. The results in Fig. 2 showed that low-dose IR ≤ 2 Gy increased the M2 polarization ratio with

a plateau observed at around 2 Gy, and further increased dose showed reverse effect with reduced M2 polarization. This trend corresponded to the bone repair results in Fig. 1. Interestingly, the irradiated healthy rats showed faster recovery of the changed polarization state (Figure S1) as compared with the cranial defect model rats. This may be due to the fact that healthy body/organ has a better ability to adjust body indicators to a normal state, which deserves our future exploration.

The results of animal experiments have also been verified at the cellular level. BMSCs were firstly inflammatory stimulated with LPS, and then subjected to different doses of IR to study the polarization profile of macrophages. The results in Fig. 4 are in line with that obtained in Fig. 3, suggesting that low-dose IR $\leq$ 2 Gy showed better efficacy on the polarization of macrophages into M2 type, while high-dose IR > 2 Gy is more likely to induce M1 polarization of macrophages. Combined with results in Fig. 1 and Fig. 3, it is inferred that low-dose IR-caused M2 polarization of macrophages is beneficial for the bone repair in the rat cranial defect model, while high-dose IR-caused M1 polarization of macrophages has the opposite effect.

Previous reports have all agreed that IR can influence the proliferation of osteoblasts, but the reported dose and final effects (positive or negative) remained controversial. [27, 30–32] In our study, the results from Fig. 5 suggested that BMSCs subjected to 2 Gy of IR showed an increased proliferation profile than the untreated control group, while the higher dose to 4 Gy showed a negative effect on their proliferation with reduced cell viability. These results suggest that the better bone repair performance of 2 Gy is related to the increased proliferation of osteoblasts, which is similar to the results offered by Liang et al. [31]

In the above results, we have shown that the IR-caused bone repair might relate to two reasons: the cell proliferation of osteoblasts and the polarization of macrophages. To further confirm this conclusion, BMSCs were cultured in OIM and subjected to different doses of IR, with/without the addition of supernatants of Raw264.7 cells irradiated with corresponding doses of IR. In line with our suggestions, the osteogenesis differentiation of BMSCs was increased with the optimal dose appearing at 2 Gy (Fig. 6A and 7A). As Fig. 5 revealed that 2 Gy of IR can increase the proliferation of BMSCs and previous studies have confirmed that proliferous BMSCs showed beneficial effects on osteogenesis and bone repair, [33, 34] it was concluded that the low-dose IR $\leq$ 2 Gy can exert a direct impact on bone repair through the increased proliferation and osteogenesis differentiation of osteoblasts. Next, the effect of IR-caused macrophages polarization on the bone repair was also studied. In the results of Fig. 6B and 7B, as compared with that of Fig. 6A and 7A, the supplement of supernatants of low-dose irradiated Raw264.7 showed a significant increase in the osteogenesis differentiation of BMSCs, indicating the strong effect of M2-polarized macrophage on bone repair. In previous studies, [18, 35] the M2 polarization of macrophages was demonstrated to secrete cytokines, including Prostaglandin E2 (PGE2) and Bone Morphogenetic Protein-2 (BMP2), to promote the proliferation and osteogenesis differentiation of osteoblasts, which represents the indirect way in the promotion of bone repair. In this experiment, we have shown that the low-dose IR $\leq$ 2 Gy can show beneficial effects on bone repair through both direct (proliferation of osteoblasts) and indirect ways (M2 polarization of macrophages), while high-dose IR > 2 Gy shows the opposite effect, and more mechanisms are worth exploring.

4. Conclusions

In this study, the rat cranial defect model revealed that low-dose IR ≤ 2 Gy significantly promotes the repair of bones, with the optimal dose lying at around 2 Gy. Low-dose IR ≤ 2 Gy induced M2 polarization of macrophages, while high-dose IR > 2 Gy was more prone to enhance M1 polarization of macrophages both *in vitro* and *in vivo* experiments. Moreover, low-dose IR ≤ 2 Gy showed enhanced proliferation of BMSCs, while high-dose IR > 2 Gy showed impaired cell viability. The osteogenesis differentiation study of BMSCs concluded that low-dose IR ≤ 2 Gy promoted osteogenesis of BMSCs by promoting cell proliferation and M2 polarization of Raw264.7, while high-dose IR > 2 Gy had the opposite effect. Our findings have revealed that low-dose IR ≤ 2 Gy promotes bone repair by indirectly promoting macrophage M2 polarization and direct osteoblast proliferation, while high-dose IR > 2 Gy has the opposite effect, which might offer inspirations for the following studies.

5. Methods

5.1 Materials

Lipopolysaccharides (LPS) was supplied by the Beyotime (Shanghai, China). NBT/BCIP tablets were supplied by Roche Diagnostics GmbH (Germany). Alizarin Red, Fluorescein diacetate (FDA) and Propidium Iodide (PI) were obtained from Solarbio Life Sciences (Beijing, China). RNA-Quick Purification Kit was obtained from ES Science (China). HiScript® II Q RT SuperMix for qPCR and AceQ® qPCR SYBR Green Master Mix were provided by Vazyme (Nanjing, China). CD68 monoclonal antibody (ED1), CD80 (B7-1) monoclonal antibody (3H5), and Goat anti-rabbit IgG (H + L) secondary antibody, PE-Cyanine 5.5 were supplied by Invitrogen (China). CD206 antibody was obtained from Santa Cruz Biotechnology (U.S.A.), Recombinant Anti-CD163 antibody was supplied by Abcam (U.S.A.). RUNX2 Rabbit mAb was supplied by Cell Signaling Technology Inc. (U.S.A.) PE-anti rat CD86 antibody, APC goat anti-mouse IgG antibody, and APC/Cyanine 7 streptavidin were obtained from Biolegend.

5.2 In vivo Osteogenesis Evaluation

All animal experiments were approved by the Nanjing Medical University Ethics Committee. Male SD rats (200–250 g) were obtained from Suzhou Sinocell Technology Ltd.

Male Sprague Dawley rats weighing 200–250 g were conducted to drilling operations to construct cranial defect models. Briefly, the rats were firstly anesthetized by intraperitoneal injection of 1% pentobarbital sodium. Subsequently, an incision with the appropriate size was made over the scalp with a scalpel for the exposure of cranium. The periosteum was splitted for the exposure of underlying bone. A trephine drill was used to create a 5-mm-diameter cranial defect on one side of the midline under continuous sterile saline irrigation. Finally, the incisions were sutured after drilling.

The rats were randomly divided into five groups after the operation (n = 3). The following treatments were conducted the next day: Group I did not receive any therapy, Group II-V received 0.5, 1, 2, 4 Gy X-ray

radiation by the linear accelerator Infinity (Elekta Corporation, Sweden), respectively. After four weeks of feeding, the rats were sacrificed, the craniums of rats were removed and fixed in formalin. Micro-computed tomography (Micro-CT, SkyScan 1176, Belgium) was used to evaluate the craniums with the following settings: voltage: 65 kV, electricity: 385 μA, Al filter: 0.5 mm. The two-dimensional (2D) and three-dimensional (3D) structures of the cranium were reconstructed using Mimics software. Bone volume/tissue volume (BV/TV) and trabecular thickness (Tb.Th) were analyzed by CT Analyser software.

5.3 Immunohistochemical staining

Immunohistochemical staining was performed to evaluate the expression of osteogenesis specific biomarkers. The immunohistochemistry of RUNX2 was performed as follows: the samples were added with cold acetone for fixation, then cultured with 5% goat serum for 1 h. After that, the sections were incubated with the primary antibody of RUNX2 for 12 h at 4°C. Finally, the secondary antibody was added and incubated for 2 h, and the samples were observed by a light microscopy.

5.4 Macrophage polarity in the blood

According to the above methodology, SD rats were modeled with cranial defect, and divided into the following five groups (n = 3) for IR on the second day: Group I served as blank controls without IR treatment, Group II-V received 0.5, 1, 2, 4 Gy X-ray IR, respectively. The day of IR was recorded as Day 0, and blood samples were taken from the orbit of each rat on Day 1, 3, 8, and 14. PBMC were separated from the blood samples by Lymphoprep according to the protocols. Separated samples were firstly labeled with CD206 antibody and recombinant anti-CD163 antibody for 30 min, then APC Goat anti-mouse IgG antibody and PE-Cyanine 5.5 were applied. After staining of CD163 and CD206, the samples were treated with CD80 monoclonal antibody and PE-anti rat CD86 antibody for 30 min, then stained with APC/Cyanine 7 streptavidin. After the labeling of cell surface antibody, the samples were fixed with 4% paraformaldehyde, permeated with intracellular staining perm wash buffer (1X), and stained with PE-anti rat CD86 antibody. Flow cytometry (BD FACSCanto II, U.S.A) was conducted to determine macrophage polarity markers in the blood samples. The sampling and detection process of the polarity changes of macrophages in healthy rats after IR were provided by supporting information.

5.5 Cell culture

Raw264.7 cells were cultured in Dulbecco's modified Eagle's medium (DMEM, high glucose) supplemented with 10% fetal bovine serum in a 37 ℃ incubator. The trypsin-EDTA solution was used to trypsinize the cells. BMSCs were cultured with DMEM (low glucose) instead of DMEM (high glucose).

5.6 RT-PCR analysis

Raw264.7 cells were seeded in 6-well plates (2×10^5 per well), and incubated for 24 h. After culturing, the cells were stimulated by lipopolysaccharide (LPS, 500 ng/mL) for 24 h, rinsed with PBS, replaced with fresh culture medium, then irradiated with various doses (0, 0.5, 1, 2, 4 Gy) of IR, and continued to incubate for 12 h. Messenger RNA (mRNA) was extracted using an RNA-quick purification kit. Then, the RNA samples were added with supermix, reverse-transcribed into complementary DNA at 50°C for 15 min,

85°C for 5 min. The qRT-PCR assay was conducted within the mixture using AceQ® qPCR SYBR Green Master Mix. Finally, the mRNA expression of macrophage M1 polarization marker genes IL-1β, iNOS, and M2 polarization marker genes BMP2, CD206, were quantified using a real-time PCR detection system (ViiA7, ThermoFisher Scientific). The relative mRNA expression levels of the target genes were normalized using GAPDH, and gene expression was calculated using the $2^{-\Delta\Delta CT}$ method. Primers used in this study are displayed in Table 1.

5.7 Cell proliferation and viability

The MTT assay was employed to determine the cell proliferation of BMSCs under different doses of IR (0, 0.5, 1, 2, 4 Gy). In brief, BMSCs cells were seeded into 96 well plates (6×10^3 cells/well) and incubated for 12 h, then treated with different doses of IR (0, 0.5, 1, 2, 4 Gy) and returned to the incubator for further cultivation (24, 48 and 72 h). MTT solution (5 mg/mL, 20 μL) was added to each well at determined time intervals for another 4 h of incubation. The medium was removed, and 200 μL of DMSO was added, which was used to dissolve the formazan crystals. The whole plate was shaken at 37 ℃ for 30 min, then subjected to measurement at 570 nm using a spectrophotometer (Epoch, BioTek). Untreated cells were selected as blank control.

BMSCs cells were seeded into 24 well plates (3×10^4 cells/well) and allowed to grow for 12 h. Then cells were treated with different doses of IR (0, 0.5, 1, 2, 4 Gy) and returned to the incubator for further cultivation of 72 h. FDA (50 μg/mL) and PI (5 μg/mL) were added to the medium for the staining of live and dead cells. Afterwards, cells were washed gently by PBS twice and subjected to observation using an inverted fluorescence microscope (iX71, Olympus).

5.8 In vitro osteogenic differentiation tests

To differentiate BMSCs into osteoblasts, different extracts were used to make up an OIM supplemented with 2 mM β-glycerophosphate, 10 nM dexamethasone, and 100 μM ascorbic acid. Standard growth medium was regarded as the control. To study the effect of macrophage polarization on the osteogenesis ability of BMSCs, the supernatants of Raw264.7 cells after irradiation with different doses after cultured for 12 hours were collected and co-cultured with BMSCs.

Six well plates were added with 0.1% gelatin solution (0.5 mL) and placed in the incubator for 1 h, then the gelatin solution was removed. Afterwards, BMSCs cells were seeded into treated-6 well plates (1×10^4 cells/well, marked as Day1). On Day3, the primary medium was replaced by a different medium, and the arranged groups were listed as follows: 1) Group I: low glucose DMEM; 2) Group II: OIM; 3) Group III-VI: OIM + 0.5, 1, 2, 4 Gy IR, respectively; 4) Group VII: OIM + supernatant of Raw264.7 cells (without radiation); 5) Group VIII-XI: OIM + 0.5, 1, 2, 4 Gy IR + supernatant of Raw264.7 cells (with the corresponding dose of radiation), respectively. The medium was replaced every three days for two weeks. On Day13, the cells were fixed with 4% paraformaldehyde for 15 min. NBT/BCIP color substrate solution was prepared by adding one tablet into 10 mL water. The cells were stained with NBT/BCIP color substrate solution for 20 min at 37°C, and observed under an optical microscopy. At Day 21, the cells were fixed with 4%

paraformaldehyde for 15 min, and stained with Alizarin Red for 20 min at 37°C. Then the samples were washed with PBS to remove nonspecific staining and directly observed by the optical microscopy.

5.9 Statistical Analysis

All data are presented as the mean value ± standard deviation from at least three independent measurements. Differences between groups were analyzed with a two-tailed non-paired Student's t-test, and mean differences with $P < 0.05$ were considered statistically significant, $P < 0.01$ represent markedly significant differences. The corresponding markers in the figures are defined as $*P < 0.05$ and $**P < 0.01$, respectively.

6. Abbreviaitons

ALP: alkaline phosphatase

BMP2: bone morphogenetic protein-2

BMSCs: rat bone marrow mesenchymal stem cells

FDA: fluorescein diacetate

IR: irradiation

LPS: lipopolysaccharides

OCN: osteocalcin

OIM: osteoblastic induction medium

OPN: osteopontin

PBMC: peripheral blood mononuclear cells

PGE2: prostaglandin E2

PI: propidium iodide

Raw264.7: mouse leukemia cells of monocyte macrophages cells

RUNX2: runt-related transcription factor 2

Declarations

7.1 Ethics approval and consent to participate

All animal experiments and care procedures were approved by the Nanjing Medical University Ethics Committee and followed the Guide for the Care and Use of Laboratory Animals (eighth edition).

7.2 Consent for publication

Not applicable.

7.3 Availability of data and materials

All materials and data supporting this study are available from the author (chenshaoqing@zju.edu.cn) upon reasonable request.

7.4 Competing interests

The authors declared no potential conflicts of interest with respect to the research, authorship, and/or publication of this article.

7.5 Funding

This work has been supported by National Natural Science Foundation of China under Grant No.81871756 and No.51672178.

7.6 Authors' contributions

Shaoqing Chen, Su Ni and Xinye Ni conceived and designed the study. Shaoqing Chen, Su Ni, Chun Liu, Mu He, Yiwen Pan, and Pengfei Cui performed the experiments. Shao-qing Chen wrote the paper. Cheng Wang and Xinye Ni reviewed and edited the manuscript.

7.7 Acknowledgements

Not applicable.

References

1. Fekete N, Erle A, Amann EM, Fürst D, Rojewski MT, Langonné A, Sensebé L, Schrezenmeier H. G. Schmidtke-Schrezenmeier. Effect of high-dose irradiation on human bone-marrow-derived mesenchymal stromal cells. Tissue Eng part C: methods. 2015;21(2):112–22.
2. Sugimoto M, Takahashi S, Toguchida J, Kotoura Y, Shibamoto Y, Yamamuro T. Changes in bone after high-dose irradiation: biomechanics and histomorphology. J Bone Joint Surg. 1991;73(3):492–7.
3. Zhang J, Qiu X, Xi K, Hu W, Pei H, Nie J, Wang Z, Ding J, Shang P, Li B. Therapeutic ionizing radiation induced bone loss: a review of in vivo and in vitro findings. Connect Tissue Res. 2018;59(6):509–22.
4. Oest ME, Franken V, Kuchera T, Strauss J, Damron TA. Long-term loss of osteoclasts and unopposed cortical mineral apposition following limited field irradiation. J Orthop Res. 2015;33(3):334–42.

5. Sugrue T, Brown JAL, Lowndes NF, Ceredig R. Multiple facets of the DNA damage response contribute to the radioresistance of mouse mesenchymal stromal cell lines. Stem Cells. 2013;31(1):137–45.
6. Wernle JD, Damron TA, Allen MJ, Mann KA. Local irradiation alters bone morphology and increases bone fragility in a mouse model. J Biomech. 2010;43(14):2738–46.
7. Xu X, Li R, Zhou Y, Zou Q, Ding Q, Wang J, Jin W, Hua G, Gao J. Dysregulated systemic lymphocytes affect the balance of osteogenic/adipogenic differentiation of bone mesenchymal stem cells after local irradiation. Stem Cell Res Ther. 2017;8(1):1–11.
8. Lau P, Baumstark-Khan C, Hellweg CE, Reitz G. X-irradiation-induced cell cycle delay and DNA double-strand breaks in the murine osteoblastic cell line OCT-1. Radiat Environ Biophys. 2010;49(2):271–80.
9. Szymczyk KH, Shapiro IM, Adams CS. Ionizing radiation sensitizes bone cells to apoptosis. Bone. 2004;34(1):148–56.
10. Colceriu-Şimon IM, Băciuţ M, Ştiufiuc RI, Aghiorghiesei A, Ţărmure V, Lenghel M, Hedeşiu M. G. Băciuţ. Clinical indications and radiation doses of cone beam computed tomography in orthodontics. Med Pharm Rep. 2019;92(4):346.
11. Fazel R, Krumholz HM, Wang Y, Ross JS, Chen J, Ting HH, Shah ND, Nasir K, Einstein AJ. B.K. Nallamothu. Exposure to low-dose ionizing radiation from medical imaging procedures. N Engl J Med. 2009;361(9):849–57.
12. Rampinelli C, De Marco P, Origgi D, Maisonneuve P, Casiraghi M, Veronesi G, Spaggiari L, M. Bellomi. Exposure to low dose computed tomography for lung cancer screening and risk of cancer: secondary analysis of trial data and risk-benefit analysis. the BMJ 356 (2017): j347.
13. Wright LE, Buijs JT, Kim HS, Coats LE, Scheidler AM, John SK, She Y, Murthy S, Ma N. H.J. Chin-Sinex. Single-limb irradiation induces local and systemic bone loss in a murine model. J Bone Miner Res. 2015;30(7):1268–79.
14. Chen M, Huang Q, Xu W, She C, Xie ZG, Mao YT, Dong QR, Ling M. Low-dose X-ray irradiation promotes osteoblast proliferation, differentiation and fracture repair. PLoS ONE. 2014;9(8):e104016.
15. Hu Y, Lau P, Baumstark-Khan C, Hellweg CE, Reitz G. X-ray induced alterations in the differentiation and mineralization potential of murine preosteoblastic cells. Adv Space Res. 2012;49(10):1422–31.
16. Park SS, Kim KA, Lee SY, Lim SS, Jeon YM, Lee JC. X-ray radiation at low doses stimulates differentiation and mineralization of mouse calvarial osteoblasts. BMB Rep. 2012;45(10):571–6.
17. Gu Q, Yang H, Shi Q. Macrophages and bone inflammation. J Orthop translation. 2017;10:86–93.
18. Pajarinen J, Lin T, Gibon E, Kohno Y, Maruyama M, Nathan K, Lu L, Yao Z. S.B. Goodman. Mesenchymal stem cell-macrophage crosstalk and bone repair. Biomaterials. 2019;196:80–9.
19. Löffler J, Sass FA, Filter S, Rose A, Ellinghaus A, Duda GN. A. Dienelt. Compromised bone repair in aged rats is associated with impaired M2 macrophage function. Front Immunol. 2019;10:2443.
20. Zhuang Z, Yoshizawa-Smith S, Glowacki A, Maltos K, Pacheco C, Shehabeldin M, Mulkeen M, Myers N, Chong R. K. Verdelis. Induction of M2 macrophages prevents bone loss in murine periodontitis

models. J Dent Res. 2019;98(2):200–8.

21. Nakao Y, Fukuda T, Zhang Q, Sanui T, Shinjo T, Kou X, Chen C, Liu D, Watanabe Y. C. Hayashi. Exosomes from TNF-α-treated human gingiva-derived MSCs enhance M2 macrophage polarization and inhibit periodontal bone loss. Acta Biomater. 2021;122:306–24.
22. Mahon OR, Browe DC, Gonzalez-Fernandez T, Pitacco P, Whelan IT, Von Euw S, Hobbs C, Nicolosi V, Cunningham KT, Mills KHG. Nano-particle mediated M2 macrophage polarization enhances bone formation and MSC osteogenesis in an IL-10 dependent manner. Biomaterials. 2020;239:119833.
23. Wu Q, Allouch A, Martins I, Modjtahedi N, Deutsch E, Perfettini JL. Macrophage biology plays a central role during ionizing radiation-elicited tumor response. Biomedical J. 2017;40(4):200–11.
24. Gough MJ, Young K. M. Crittenden. The Impact of the Myeloid Response to Radiation Therapy. Clin Dev Immunol. 2013;2013:281958.
25. Sinder BP, Pettit AR, McCauley LK. Macrophages: their emerging roles in bone. J Bone Miner Res. 2015;30(12):2140–9.
26. Cho SW. Role of osteal macrophages in bone metabolism. J Pathol translational Med. 2015;49(2):102–4.
27. Reinke S, Geissler S, Taylor WR, Schmidt-Bleek K, Juelke K, Schwachmeyer V, Dahne M, Hartwig T, Akyüz L. C. Meisel. Terminally differentiated CD8 + T cells negatively affect bone regeneration in humans. Sci Transl Med. 2013;5(177):177ra36.
28. Schlundt C, El Khassawna T, Serra A, Dienelt A, Wendler S, Schell H, van Rooijen N, Radbruch A, Lucius R. S. Hartmann. Macrophages in bone fracture repair: their essential role in endochondral ossification. Bone. 2018;106:78–89.
29. Mantovani A, Biswas SK, Galdiero MR, Sica A. M. Locati. Macrophage plasticity and polarization in tissue repair and remodelling. J Pathol. 2013;229(2):176–85.
30. Nicolay NH, Sommer E, Lopez R, Wirkner U, Trinh T, Sisombath S, Debus J, Ho AD, Saffrich R, Huber PE. Mesenchymal stem cells retain their defining stem cell characteristics after exposure to ionizing radiation. Int J radiation oncology-biology-physics. 2013;87(5):1171–8.
31. Liang X, So YH, Cui J, Ma K, Xu X, Zhao Y, Cai L, Li W. The low-dose ionizing radiation stimulates cell proliferation via activation of the MAPK/ERK pathway in rat cultured mesenchymal stem cells. J Radiat Res. 2011;52(3):380–6.
32. Wang Y, Zhu G, Wang J, Chen J. Irradiation alters the differentiation potential of bone marrow mesenchymal stem cells. Mol Med Rep. 2016;13(1):213–23.
33. Dallari D, Fini M, Stagni C, Torricelli P, Nicoli Aldini N, Giavaresi G, Cenni E, Baldini N, Cenacchi A. A. Bassi. In vivo study on the repair of bone defects treated with bone marrow stromal cells, platelet-rich plasma, and freeze-dried bone allografts, alone and in combination. J Orthop Res. 2006;24(5):877–88.
34. Huang Y, He B, Wang L, Yuan B, Shu H, Zhang F, Sun L. Bone marrow mesenchymal stem cell-derived exosomes promote rotator cuff tendon-bone repair by promoting angiogenesis and regulating M1 macrophages in rats. Stem Cell Res Ther. 2020;11(1):1–16.

35. Zhao SJ, Kong FQ, Jie J, Li Q, Liu H, Xu AD, Yang YQ, Jiang B, Wang DD, Zhou ZQ, Tang PY, Chen J, Wang Q, Zhou Z, Chen Q, Yin GY, Zhang HW, J. Fan. Macrophage MSR1 promotes BMSC osteogenic differentiation and M2-like polarization by activating PI3K/AKT/GSK3β/β-catenin pathway. Theranostics 10(1) (2020): 17–35.

Table

Table 1 Primers used for RT-PCR

Gene	Primer	Sequence
IL-1β	Forward	TCGCAGCAGCACATCAACAAGAG
	Reverse	AGGTCCACGGGAAAGACACAGG
iNOS	Forward	CTGCAGCACTTGGATCAGGAACCTG
	Reverse	GGAGTAGCCTGTGTGCACCTGGAA
BMP2	Forward	GGGACCCGCTGTCTTCTAGT
	Reverse	TCAACTCAAATTCGCTGAGGAC
CD206	Forward	AGGACGAAAGGCGGGATG
	Reverse	TTGGGTTCAGGAGTTGTTGTG
GADPH	Forward	AGGTCGGTGTGAACGGATTTG
	Reverse	TGTAGACCATGTAGTTGAGGTCA

Figures

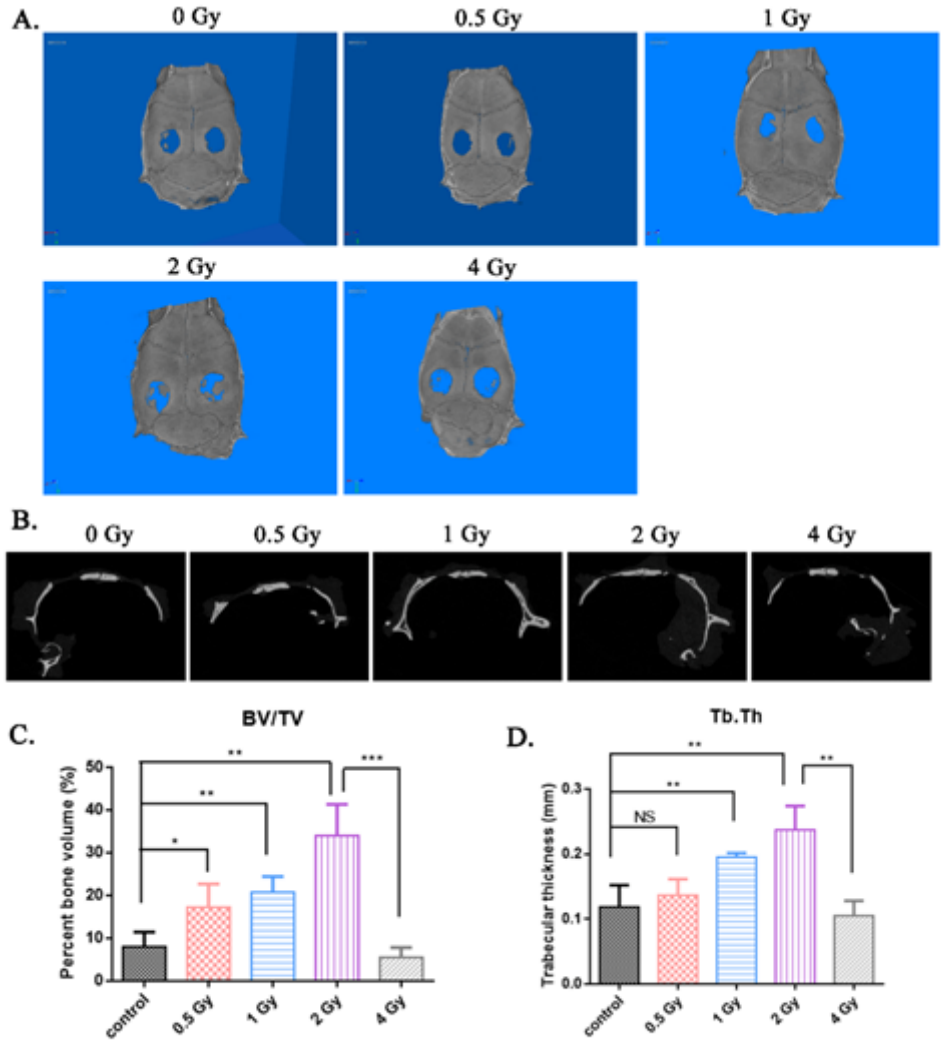

Figure 1

Micro-CT analysis of the cranium after different doses of IR for 28 days. (A) 3D-reconstruction of cranium in different groups. (B) Sagittal view of rat cranial defect in different groups. (C, D) Micro-CT analysis of BV/TV (C) and Tb.Th (D). NS: no significant difference, *P<0.05, **P<0.01, ***P<0.001. The error bars in the graphs represent the standard deviation (n = 3).

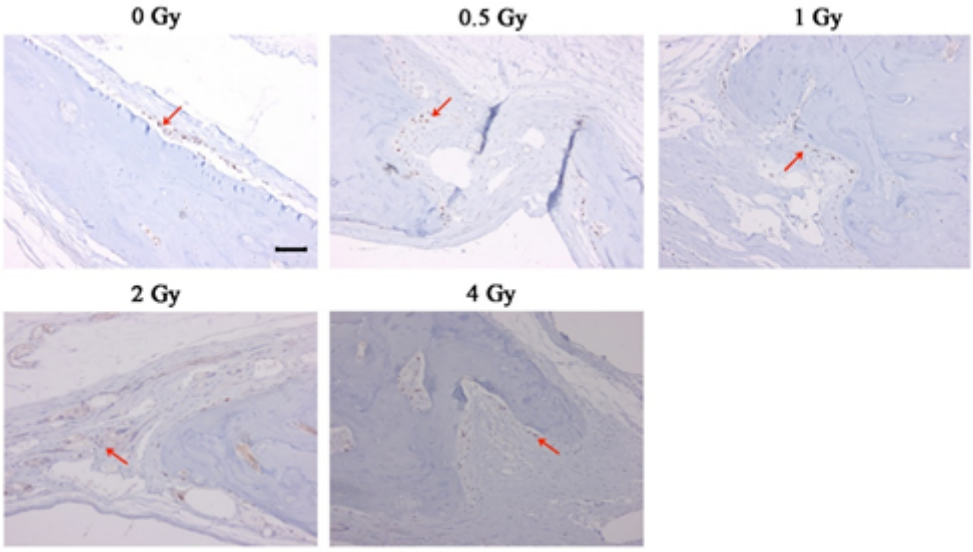

Figure 2

Immunohistochemical staining of RUNX2 (200×) in cranium after different doses of IR for 28 days. Brown precipitation represents positive staining. Scale bars, 100 μm.

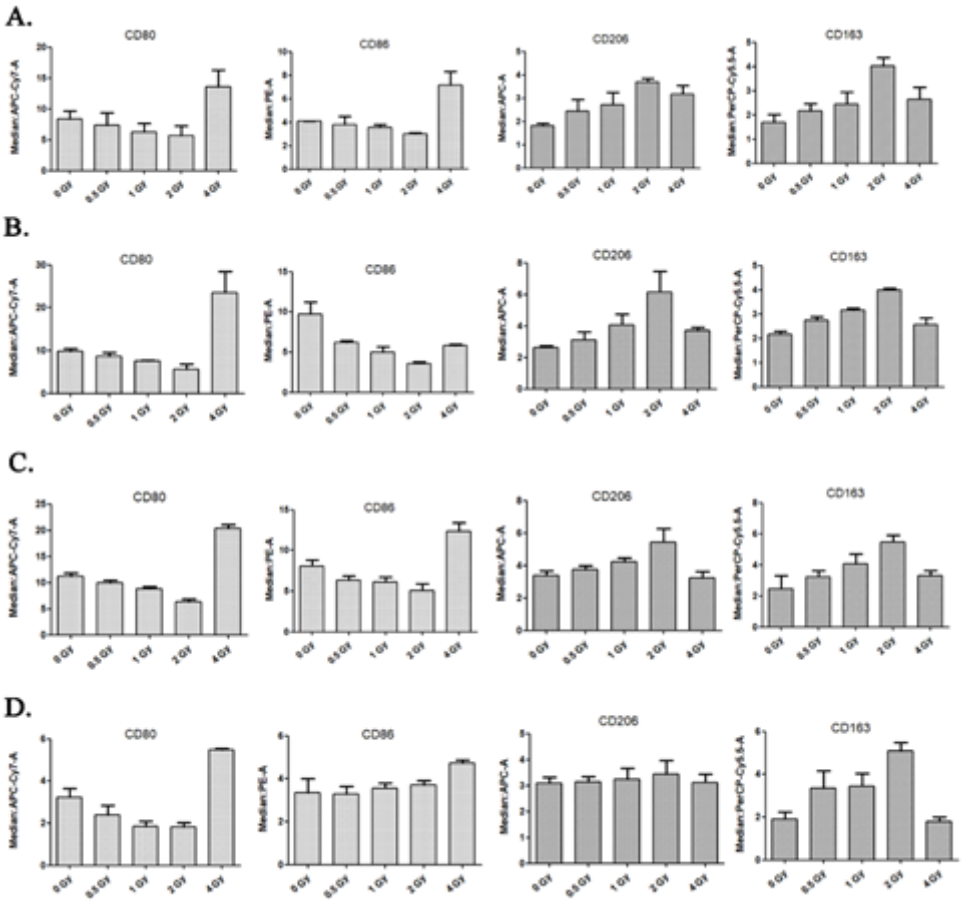

Figure 3

Flow cytometric quantitative results of macrophage M1 and M2 markers from the blood samples of the bone defect model rats on Day1 (A), Day3 (B), Day8 (C) and Day14 (D) after IR. The error bars in the graphs represent the standard deviation (n = 3).

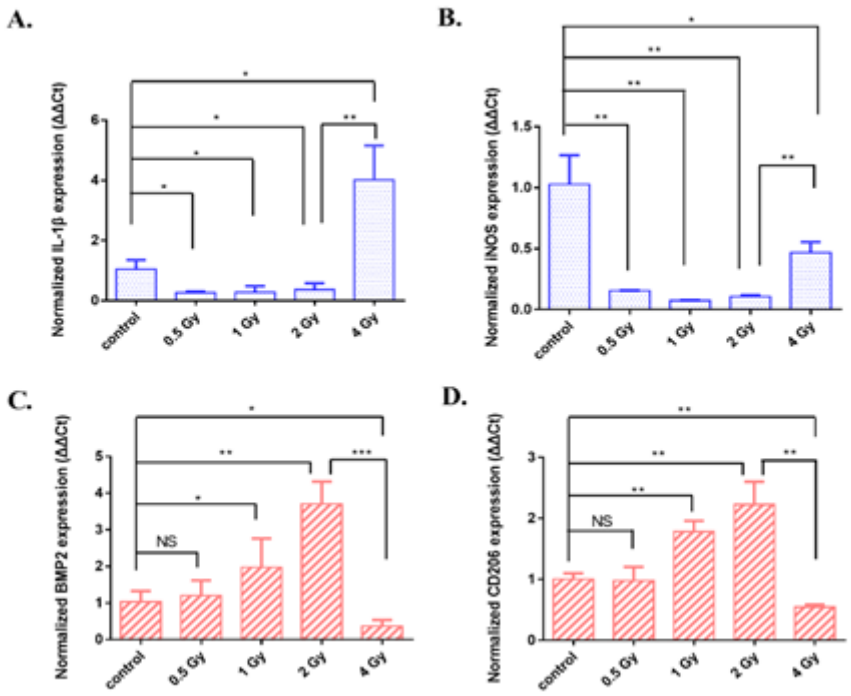

Figure 4

Raw264.7 cells were exposed to LPS inflammatory stimulation (500 ng/mL, 24 h), then irradiated by different doses of IR, and cultured for 24 h. RT-PCR was used to determine the intracellular mRNA expression of M1 markers (A) IL-1β, (B) iNOS, and M2 markers (C) BMP2, (D) CD206. NS: no significant difference, *P<0.05, **P<0.01, ***P<0.001. The error bars in the graphs represent the standard deviation (n = 3).

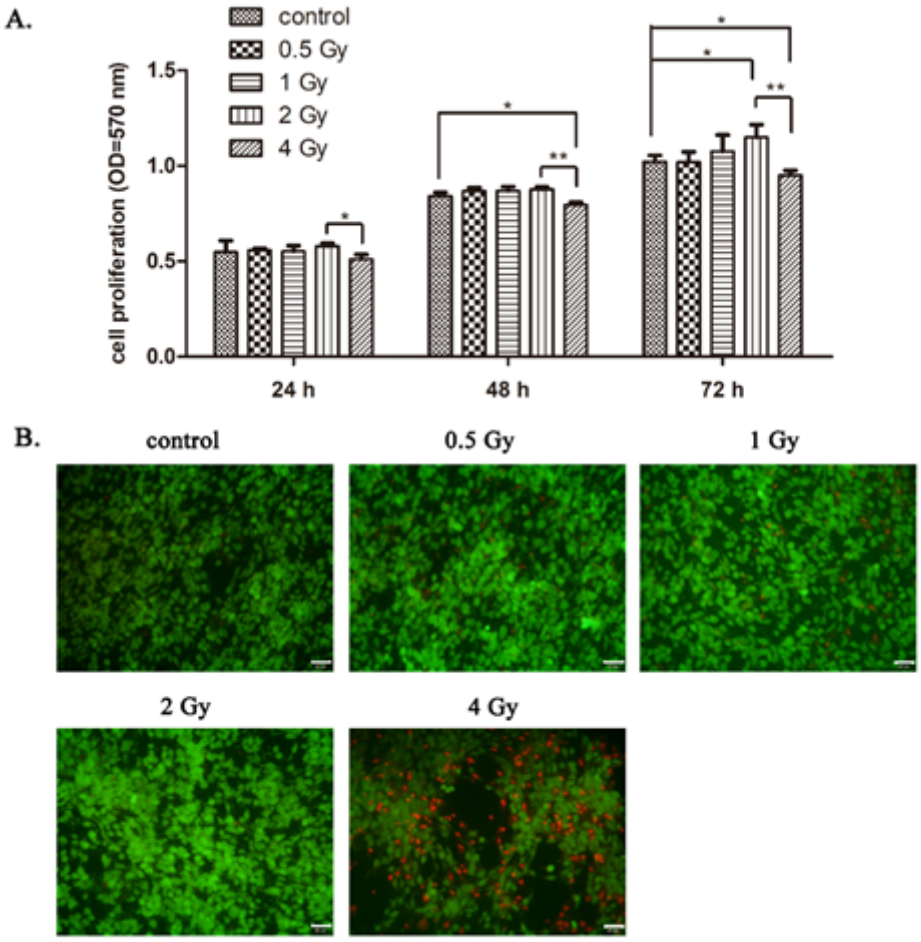

Figure 5

The effects of different doses of IR on the proliferation of BMSCs. (A) MTT assay of BMSCs at 24, 48, and 72 h post-IR. (B) BMSCs were stained with FDA/PI at 72 h post-IR. Green: FDA, red: PI. *P<0.05, **P<0.01. The error bars in the graphs represent the standard deviation (n = 3). Scale bar, 50 μm.

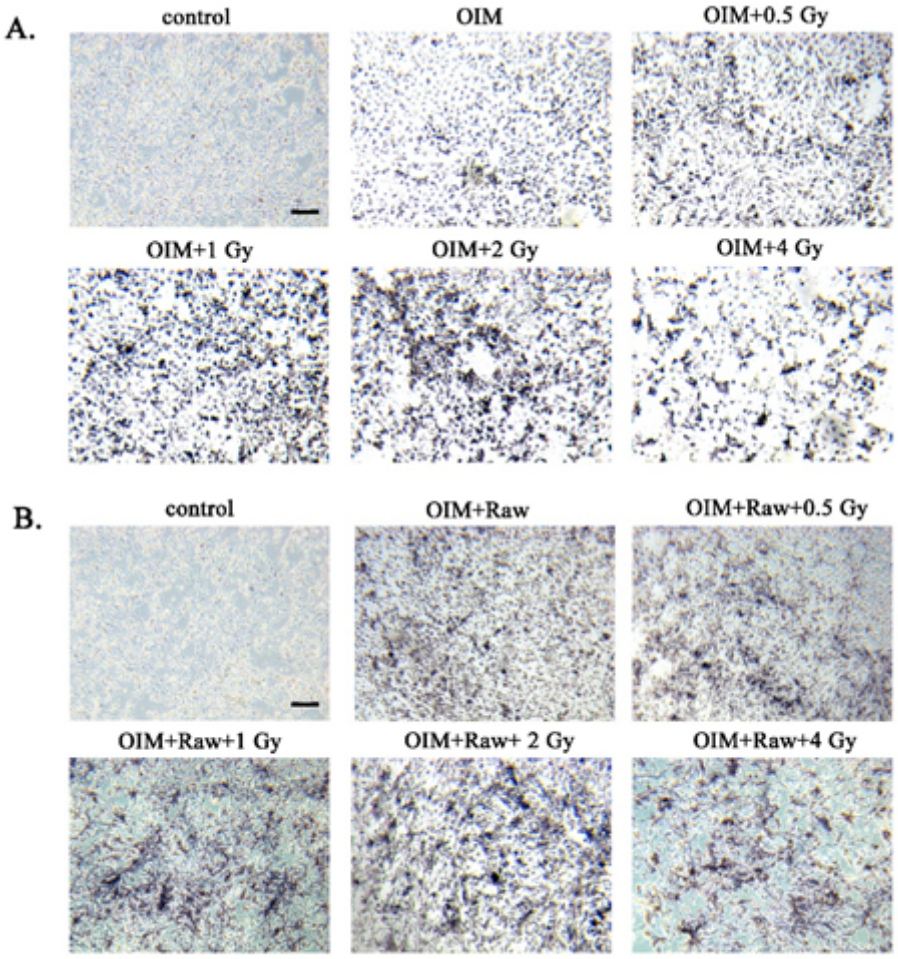

Figure 6

ALP staining of BMSCs with different treatments at day 13. (A) BMSCs treated with OIM and different doses of IR. (B) BMSCs treated with OIM, different doses of IR, and supernatants of Raw264.7 cells irradiated with corresponding doses IR. Scale bar, 100 μm.

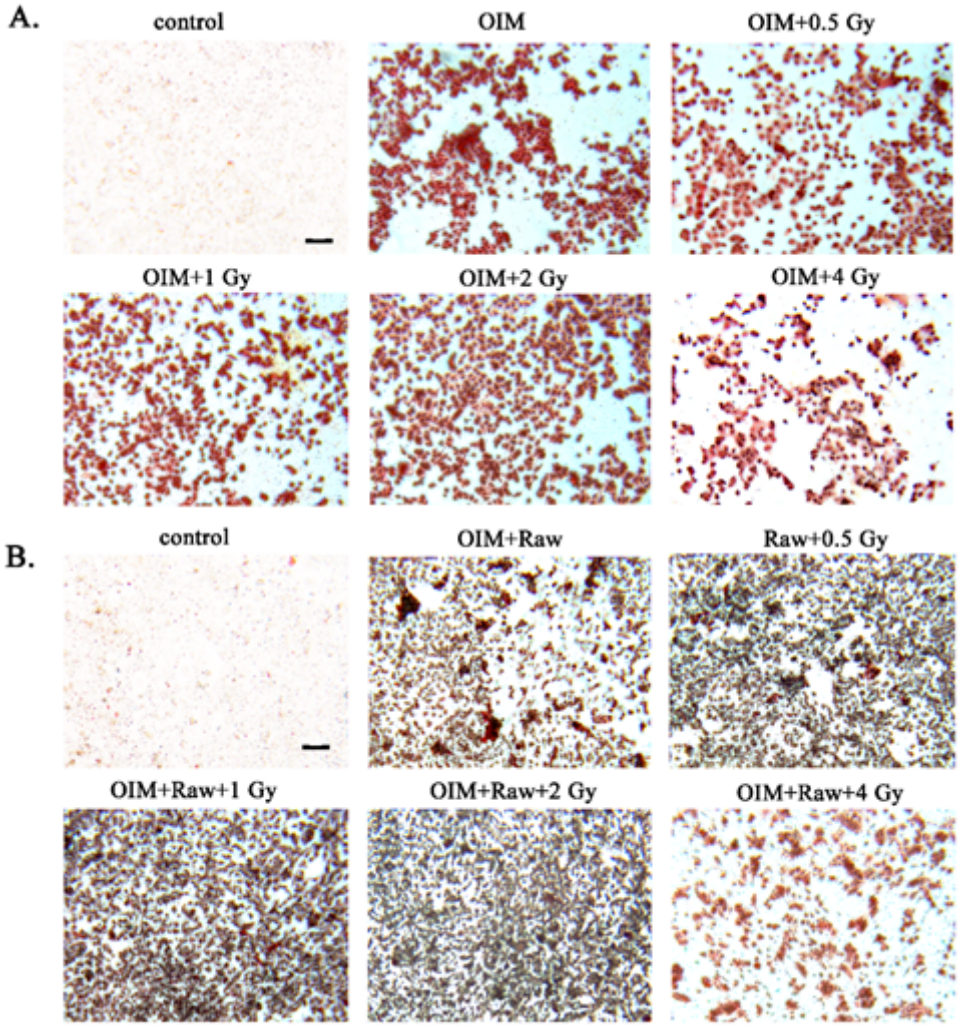

Figure 7

AR staining of BMSCs with different treatments at day 21. (A) BMSCs treated with OIM and different doses of IR. (B) BMSCs treated with OIM, different doses of IR, and supernatants of Raw264.7 cells irradiated with corresponding doses of IR. Scale bar, 100 μm.

Supplementary Files

This is a list of supplementary files associated with this preprint. Click to download.

- SupportingInformation.docx